

Supporting Information

Incorporating electron-deficient bipyridinium chromophores to make multiresponsive metal-organic frameworks

Ning-Ning Yang, Jia-Jia Fang, Qi Sui, En-Qing Gao*

†Shanghai Key Laboratory of Green Chemistry and Chemical Processes, School of Chemistry and Molecular Engineering, East China Normal University, Shanghai 200062 (P. R. China).

Email: eqgao@chem.ecnu.edu.cn.

Contents

Materials and methods	S-2
Table S1 Electrochemical and energetic data for UiO-67-DQ-X and UiO-67-MQ-X.....	S-3
Figure S1 IR spectra of the MOFs before and after modification.....	S-4
Figure S2 ¹ H NMR spectra of UiO-67-bpy and UiO-67-DQ.....	S-4
Figure S3 SEM pictures of UiO-67-DQ in different resolutions.....	S-5
Figure S4 TGA of UiO-67-bpy and UiO-67-DQ.....	S-5
Figure S5 IR spectra of UiO-67-DQ and UiO-67-MQ before and after ion-exchange.....	S-6
Figure S6 PXRD patterns of UiO-67-MQ-X.....	S-7
Figure S7 PXRD patterns of UiO-67-DQ after consecutive exchange cycles.....	S-7
Figure S8 The color change of UiO-67-MQ-X before and after irradiation.....	S-8
Figure S9 UV-vis spectra of UiO-67-MQ-X.....	S-8
Figure S10 Milliken plots including both UiO-67-DQ-X and UiO-67-MQ-X.....	S-9
Figure S11 UV-vis spectra of UiO-67-MQ-X after irradiation.....	S-9
Figure S12 Fluorescence spectra of different MOFs and related ligands.....	S-10
Figure S13 Fluorescence spectra of UiO-67-MQ-X before and after irradiation.....	S-10
Figure S14 Cyclic voltammograms of UiO-67-MQ-X.....	S-11
Figure S15 PXRD patterns of the solid isolated and fluorescence spectra of the superantant.....	S-11
Figure S16 Color response of UiO-67-DQ/EtOH suspensions to different anions.....	S-12
Figure S17 Color response and fluorescence intensity of UiO-67-MQ/EtOH.....	S-12
Figure S18 Fluorescence spectra and the Stern–Volmer plots for detection of I ⁻	S-13
Figure S19 Fluorescence spectra of UiO-67-DQ for the NOR gate.....	S-13
Figure S20 Fluorescence spectra of UiO-67-MQ for INHIBIT and IMPLICATION gates.....	S-14
Figure S21 UiO-67-MQ-based 3-input logic operations integrating INHIBIT and OR/NOR gates.....	S-14
Figure S22 Fluorescence spectra of UiO-67-MQ for the 5-input integrated logic operation.....	S-15
References	S-15

Materials and methods.

All chemicals were used as purchased. H₂bpydc¹, UiO-67-bpy², UiO-67-MQ³ and EDT⁴ were synthesized according to literature procedures. General physical methods are described in the supporting information.

Physical methods. ¹H NMR spectra were recorded on a Bruker Advance 400 MHz spectrometer. The FT-IR spectra were recorded in the range 500-4000 cm⁻¹ using KBr pellets on a Nicolet NEXUS 670 spectrophotometer. Powder X-ray diffraction (PXRD) at ambient pressure was recorded on a Rigaku D/Max-2500 diffractometer at 35kV, 25mA for a Cu-target tube and a graphite monochromator. UV-vis diffuse reflectance spectra were measured using a SHIMADZU UV-2700 spectrophotometer, with BaSO₄ plates as references (100% reflection). Fluorescence spectra were recorded on a Hitachi F-4500 spectrofluorometer. Scanning electron microscopy (SEM) was performed on a Hitachi S-4800 microscope. Nitrogen adsorption and desorption isotherm measurements were performed on a Micromeritics ASAP2020 analyzer at 77K. Thermogravimetric analysis (TGA) experiments were performed on a NETZSCH STA 449 F3. Room-temperature X-band electron spin resonance (ESR) spectroscopy was performed using a Bruker Elexsys580 spectrometer with a 100 kHz magnetic field.

Electrochemical methods. Cyclic voltammetry (CV) was carried out with a CHI 604E workstation (Shanghai CH Instrument Company, China) with a three-electrode system, where the counter, reference and working electrodes are a platinum wire, an Ag/AgCl electrode and a modified glassy carbon electrode (GCE), respectively. For preparation of the modified GCE, a bare GCE (Φ3mm) was polished with slurry alumina (1.0, 0.3 and 0.05 mm, respectively), sonicated and washed thoroughly with ethanol and double deionized water. 1 mg of a MOF was dispersed in the mixture of 0.1mL deionized water and 10 μL Nafion (5%) by ultrasonication to form a suspension. Then 2.5 μL suspension was drop-coated onto the GCE and then the electrode was dried in air.

Preparation of anion test papers. The filter paper was cut into strips of 0.5 × 2 cm². The strips were dipped into a dispersion of UiO-67-DQ-TfO in water (10 mg/mL, uniformly dispersed by ultrasonication) for a few seconds and then left to dry at room temperature. The dip-coating and drying procedure was repeated for three times. No indication of falling off was observed during the use of the test paper.

Table S1 Formal potentials, onset potentials of the first reduction peaks, HOMO and LUMO energies and band gaps of UiO-67-DQ-X and UiO-67-MQ-X. ^a

	E_1	E_2	$E_{\text{Onset}}^{\text{Red}}$	E_g	LUMO	HOMO
	[V]	[V]	[V]	[eV] ^b	[eV] ^c	[eV] ^d
UIO-67-DQ-Cl ⁻	-0.335	-0.718	-0.231	3.30	-4.47	-7.77
UIO-67-DQ-Br ⁻	-0.345	-0.721	-0.245	2.94	-4.46	-7.40
UIO-67-DQ-SCN ⁻	-0.347	-0.710	-0.246	2.36	-4.45	-6.81
UIO-67-DQ-I ⁻	-0.349	-0.706	-0.251	2.19	-4.45	-6.64
UIO-67-DQ-TfO ⁻	-0.363	-0.711	-0.260	3.47	-4.44	-7.91
UIO-67-MQ-Cl ⁻	-0.670	-1.017	-0.546	3.48	-4.15	-7.63
UIO-67-MQ-Br ⁻	-0.666	-1.040	-0.518	3.38	-4.18	-7.56
UIO-67-MQ-SCN ⁻	-0.662	-1.037	-0.559	2.93	-4.14	-7.07
UIO-67-MQ-I ⁻	-0.654	-1.010	-0.542	2.65	-4.16	-6.81
UIO-67-MQ-TfO ⁻	-0.651	-1.028	-0.463	3.51	-4.24	-7.75

^a Potentials are reported vs Ag/AgCl. ^b Band gap calculated from the onset wavelength (λ_{onset} , nm) of the UV-vis spectrum using $E_g = 1240/\lambda_{\text{onset}}$.⁵ For the compounds with appreciable CT absorption, E_g is assumed to be the CT transition energy (Δ_{CT}), which is used in Figures 4 and S10. ^c Calculated using $E_{\text{LUMO}} = -(E_{\text{Onset}}^{\text{Red}} + 4.70)(\text{eV})$.⁶ ^d HOMO = LUMO - E_g .

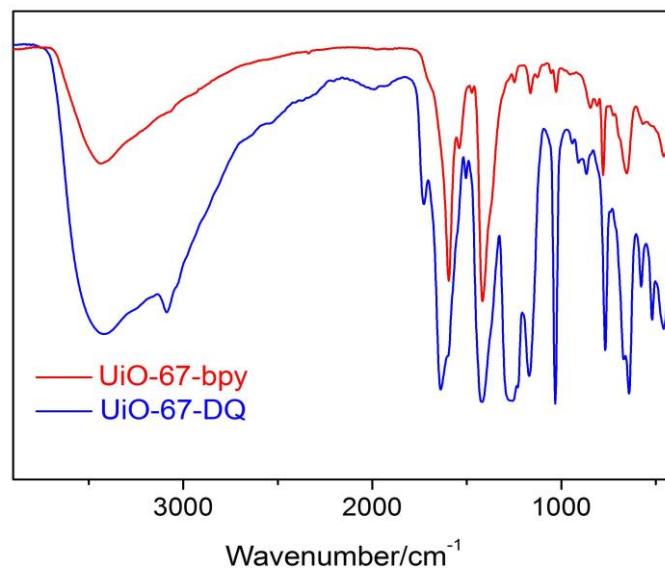


Figure S1. IR spectra of the MOFs before and after modification.

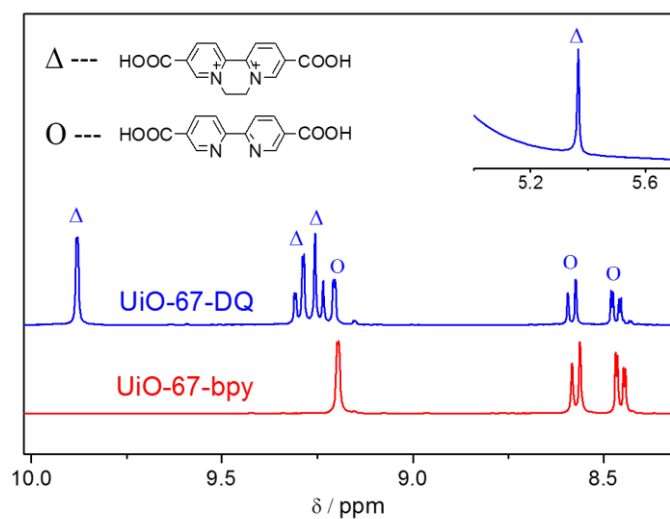


Fig S2. ^1H NMR spectra of UiO-67-bpy and UiO-67-DQ. The spectra were recorded with the solutions obtained by digesting the solids with HF (aq.)/ d_6 -DMSO (1/40, v/v).

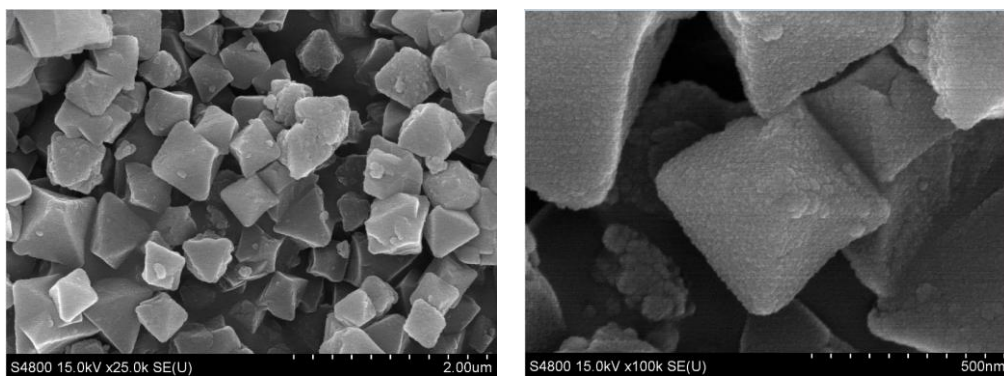


Figure S3. SEM pictures of UiO-67-DQ in different resolutions.

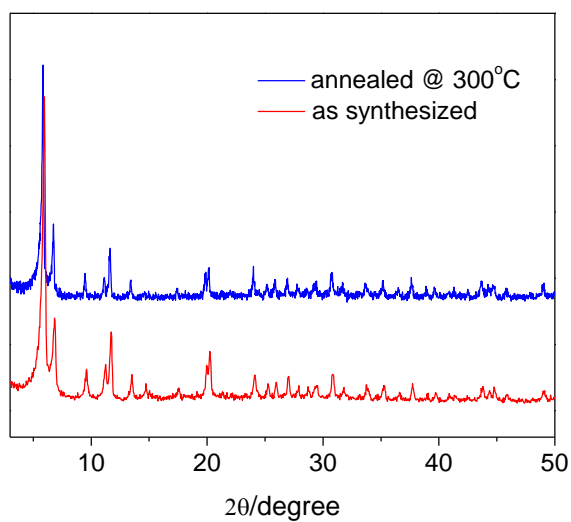
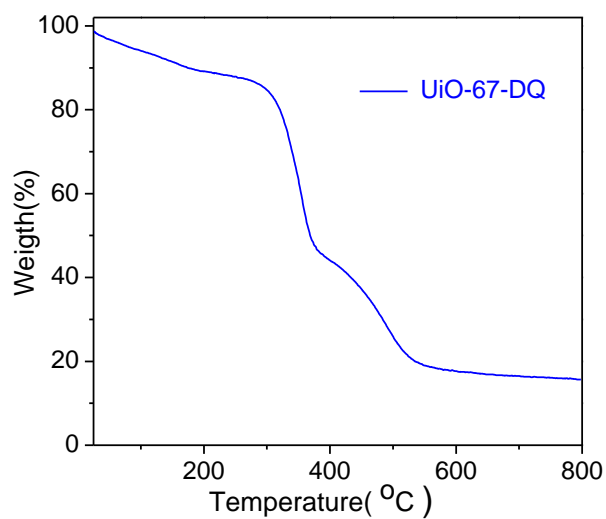


Figure S4. Top: Thermogravimetric plot of UiO-67-DQ. Bottom: PXRD profiles for UiO-67-DQ (as synthesized and after annealing at 300°C for 30 min).

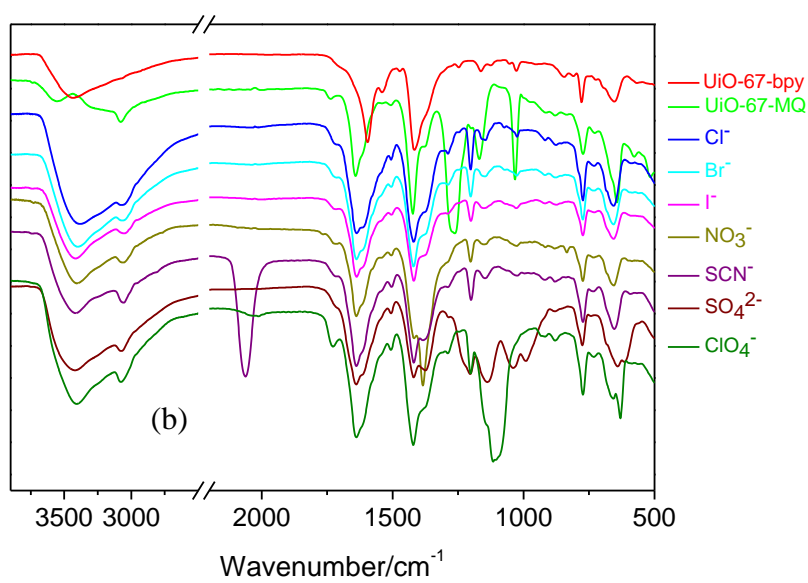
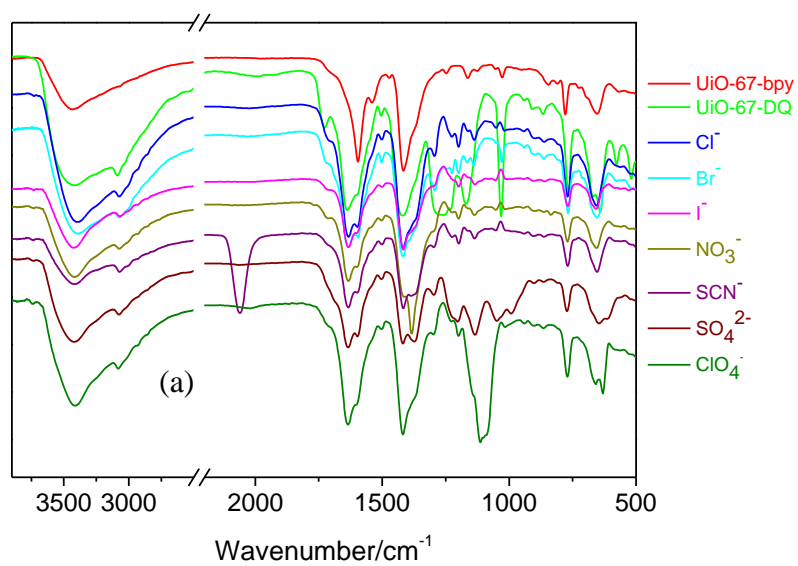


Figure S5. IR spectra of (a) UiO-67-DQ and (b) UiO-67-MQ before and after ion-exchange.

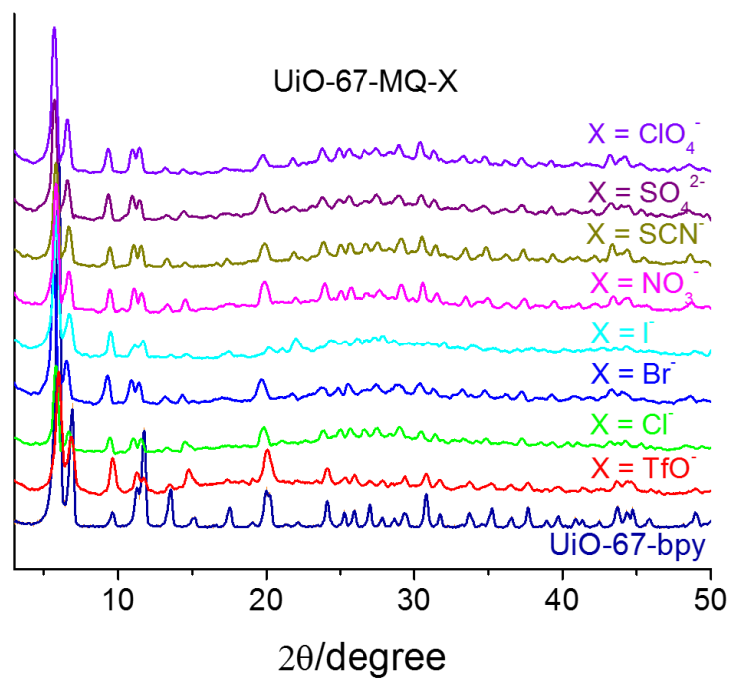


Figure S6. PXRD patterns of UiO-67-MQ-X.

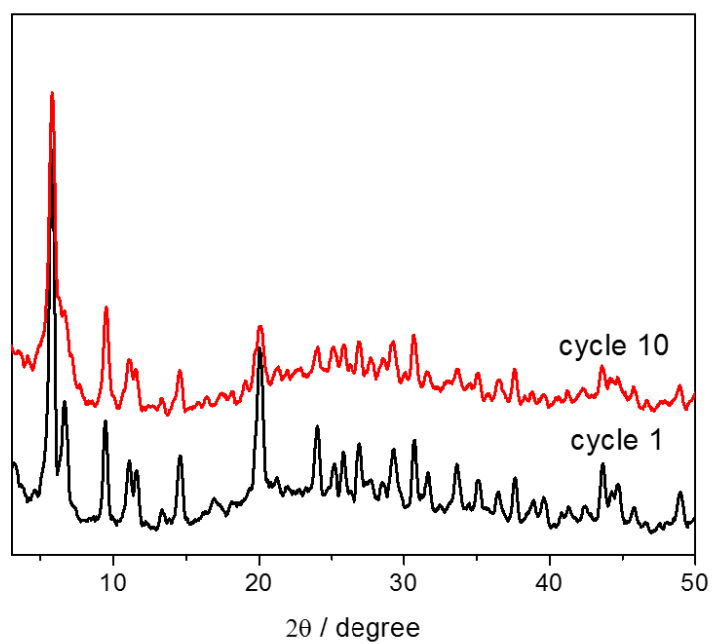


Figure S7. PXRD patterns of UiO-67-DQ after consecutive exchange cycles between CF_3SO_3^- and I^- .



Figure S8. The color change of UiO-67-MQ-X before and after illuminated under a xenon lamp.

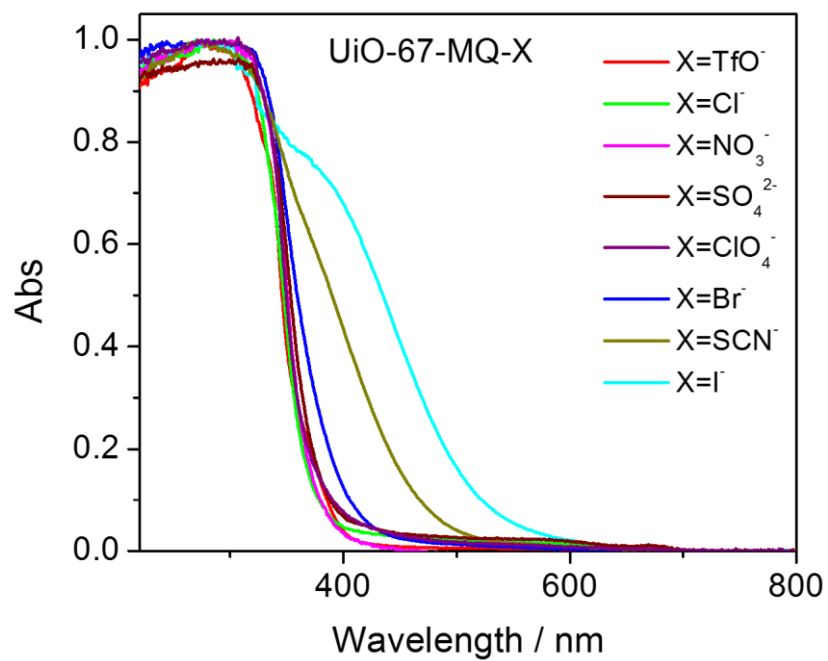


Figure S9. UV-vis spectra of UiO-67-MQ-X.

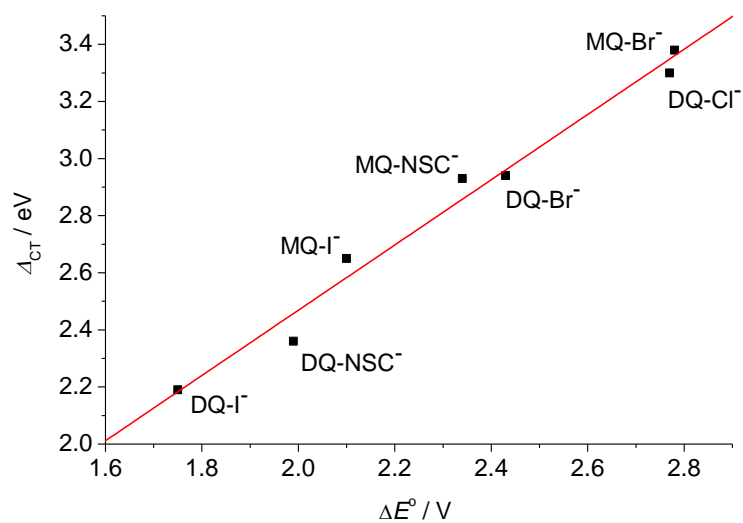


Figure S10. Milliken plots including both UiO-67-DQ-X and UiO-67-MQ-X (X = (pseudo)halides). Δ_{CT} is the CT transition energy, $\Delta E^\circ = E^\circ(X^-/X) - E^\circ(Q^{2+}/Q^\bullet)$ with Q = MQ and DQ.

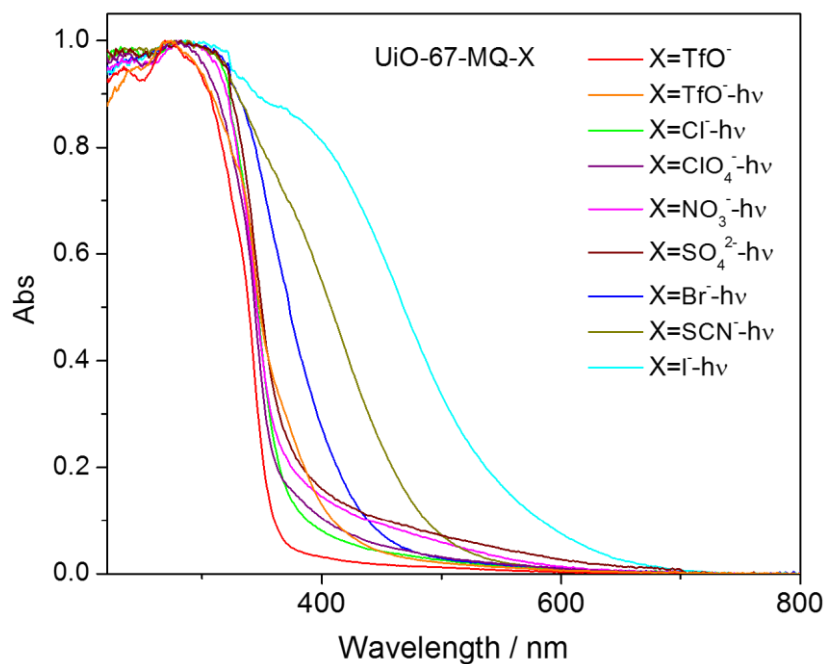


Figure S11. UV-vis spectra of UiO-67-MQ-X after illuminated under a xenon lamp.

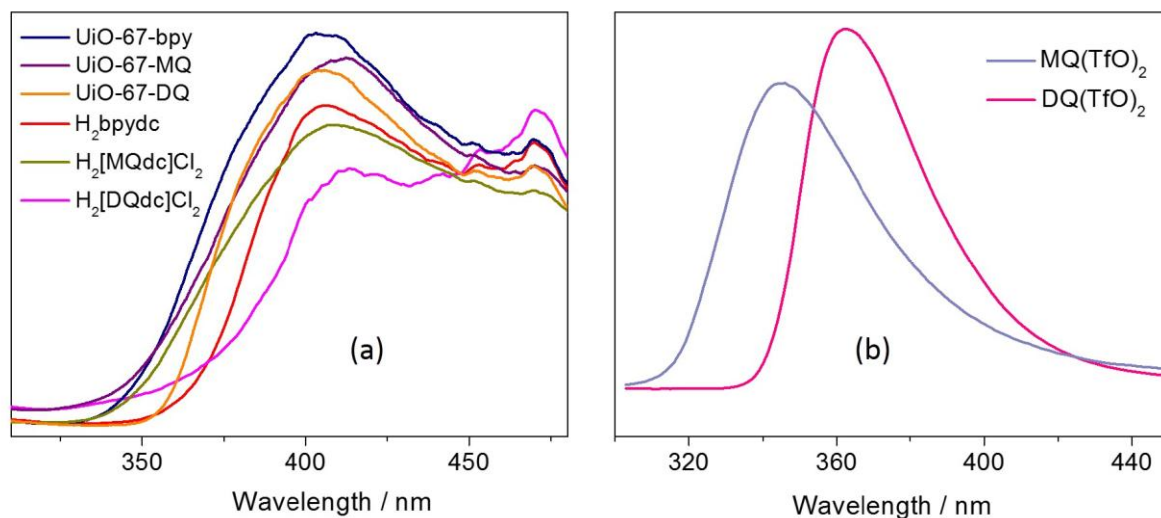


Figure S12 (a) Fluorescence spectra of different MOFs and their ligands. H₂bpydc = 2,2'-bipyridyl-5,5'-dicarboxylic acid, [H₂MQdc]Cl₂ = 1,1'-dimethyl-5,5'-dicarboxy-2,2'-bipyridinium dichloride, [H₂DQdc]Cl₂ = 1,1'-ethylene-5,5'-dicarboxy-2,2'-bipyridinium dichloride. (b) Fluorescence spectra of MQ(TfO)₂ and DQ(TfO)₂.

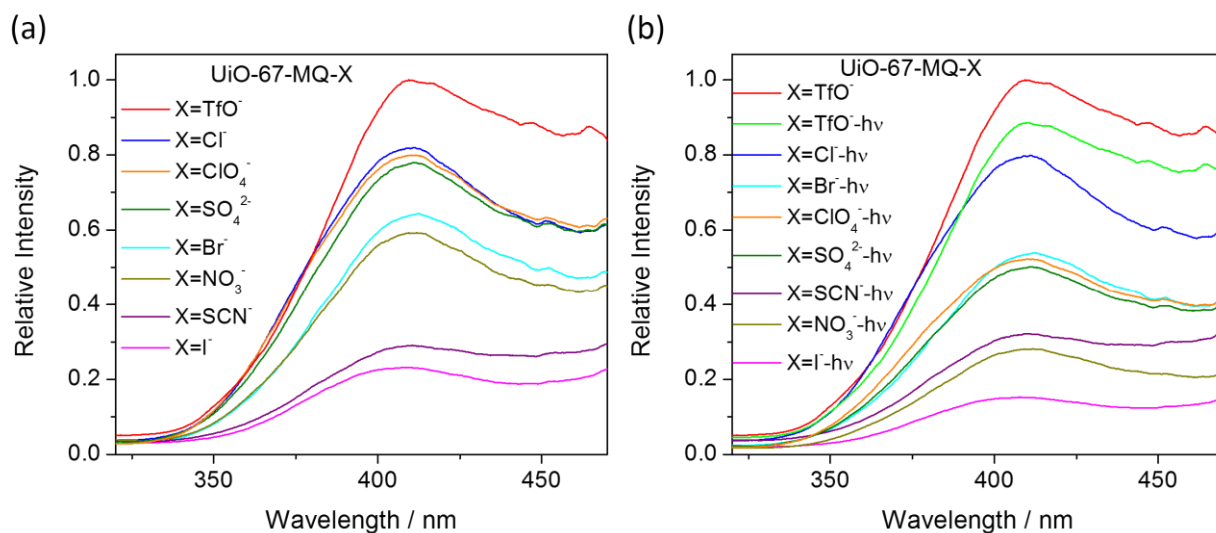


Figure S13 Fluorescence spectra of UiO-67-MQ-X before (a) and after (b) irradiation.

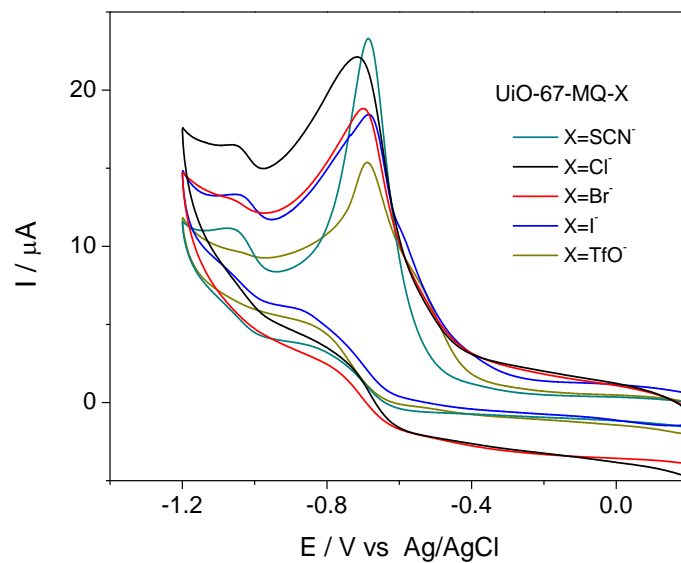


Figure S14. Cyclic voltammograms of UiO-67-MQ-X in corresponding salt solution (0.1 M, KCl, KBr, KI, KSCN and NaOTf). Scan rate $\nu = 100 \text{ mV s}^{-1}$.

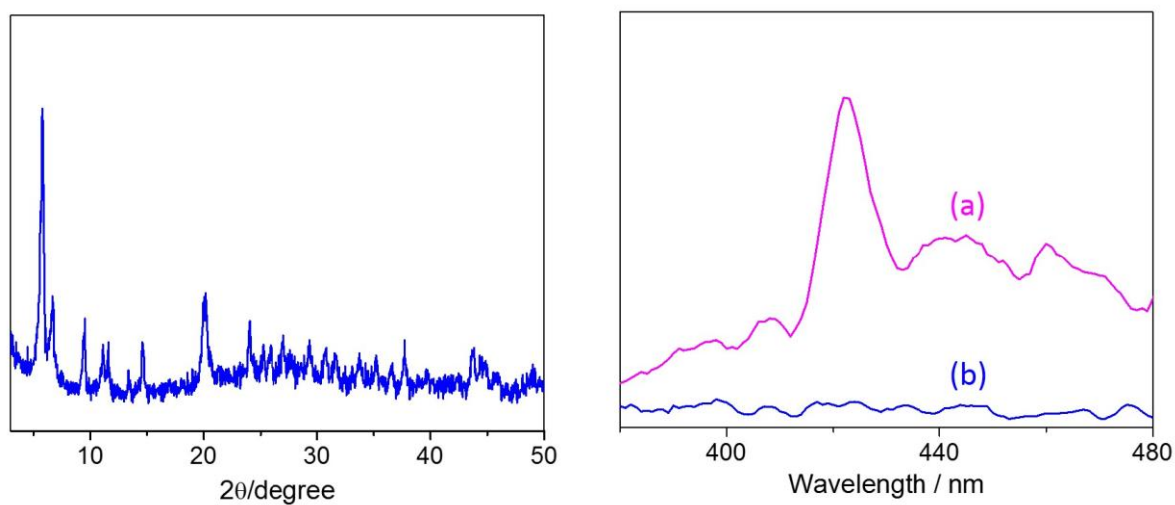


Figure S15. Left: PXRD pattern of the solid centrifuged from the UiO-67-DQ/water suspension. Right: Fluorescence spectra of the UiO-67-DQ/water suspension (a) and the supernatant after centrifugation (b).

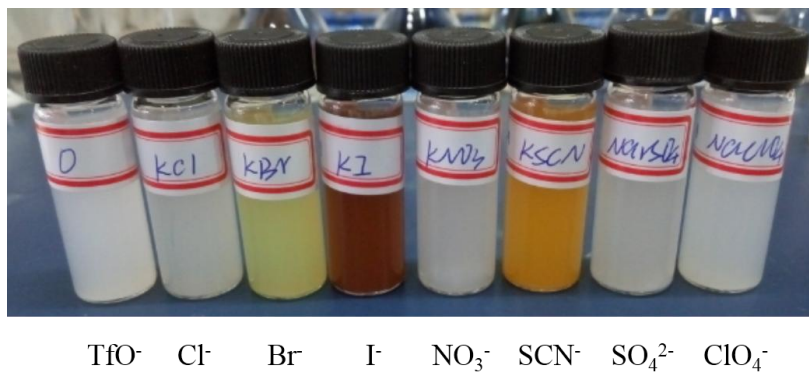


Figure S16. Color response of UiO-67-DQ/EtOH suspensions to different anions.

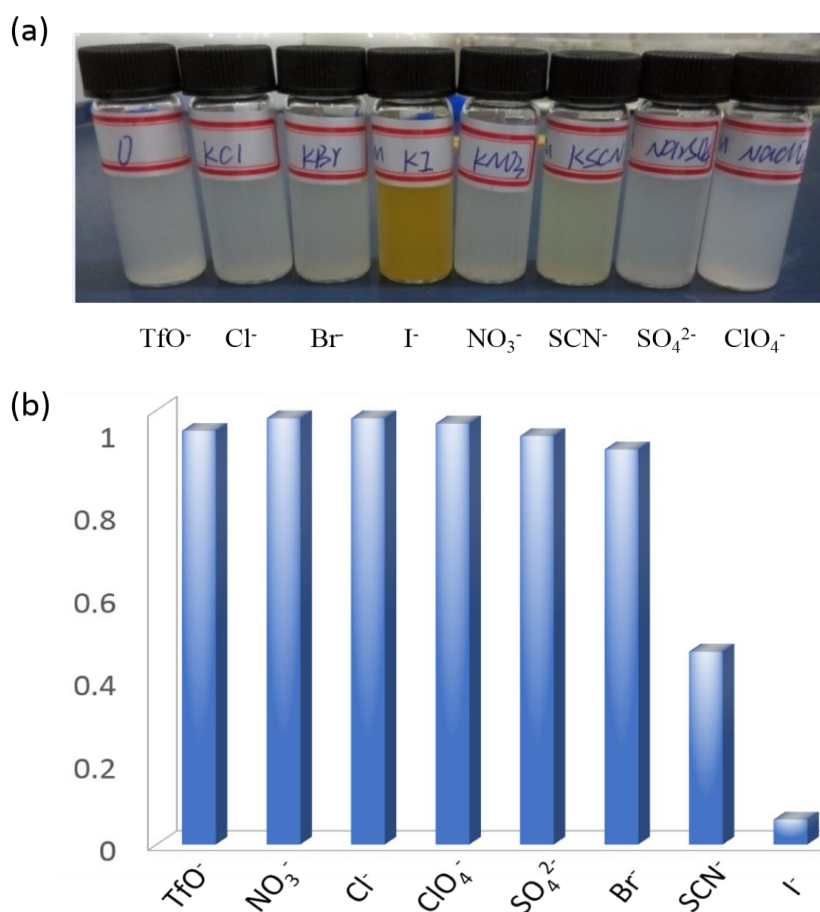


Figure S17. (a) Color response of UiO-67-MQ/EtOH suspensions to anions. (b) Fluorescence intensity (423 nm) of UiO-67-MQ/EtOH dispersions in response to anions (4×10^{-3} M).

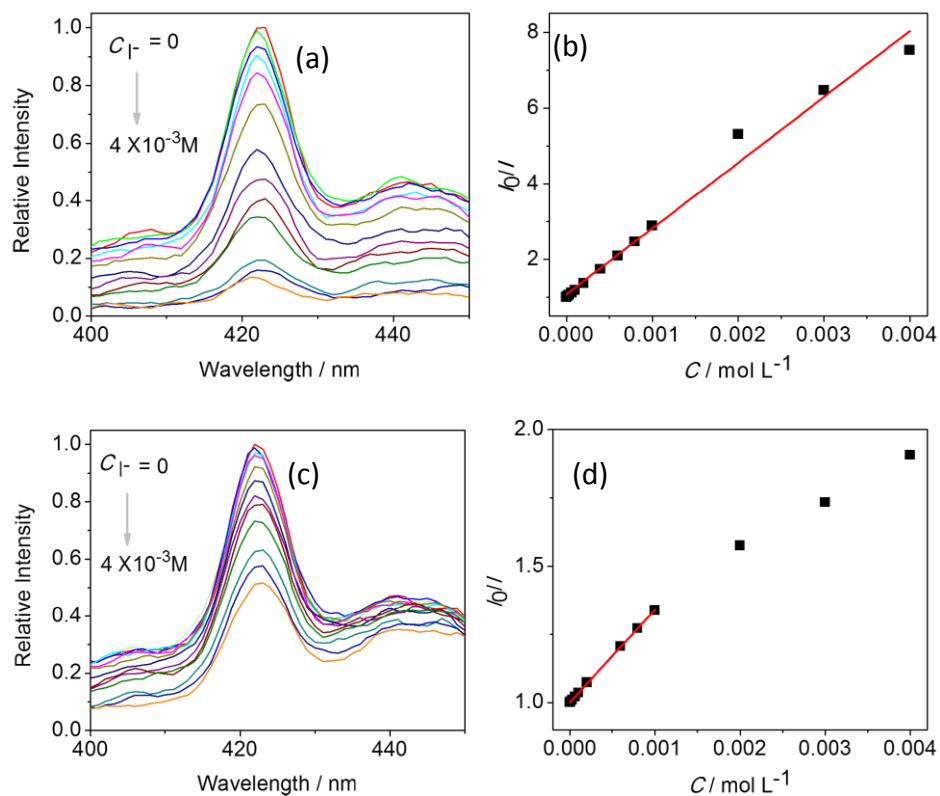


Figure S18. Fluorescence spectra of the UiO-67-DQ/H₂O (a) and UiO-67-MQ/H₂O (c) dispersions in response to KI. The variation of I_0/I (at 423 nm) of UiO-67-DQ/H₂O (b) and UiO-67-MQ/H₂O (d) with the concentration of iodide.

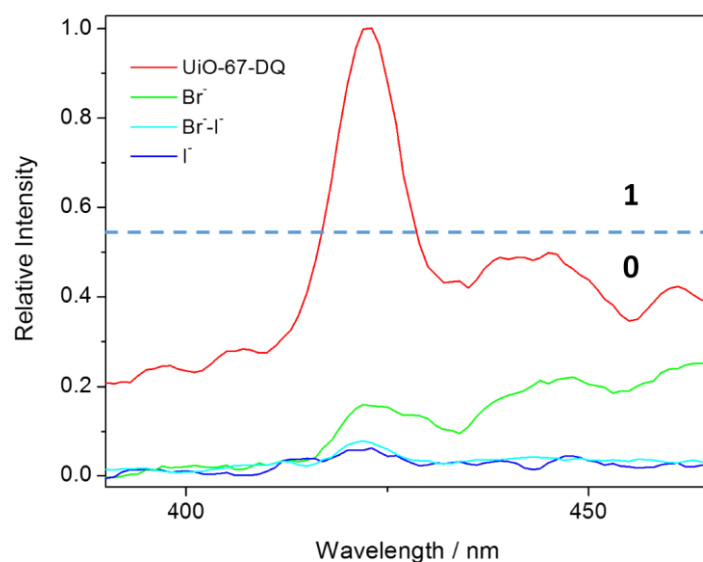


Figure S19. Fluorescence spectra of UiO-67-DQ for different input combinations of the NOR gate.

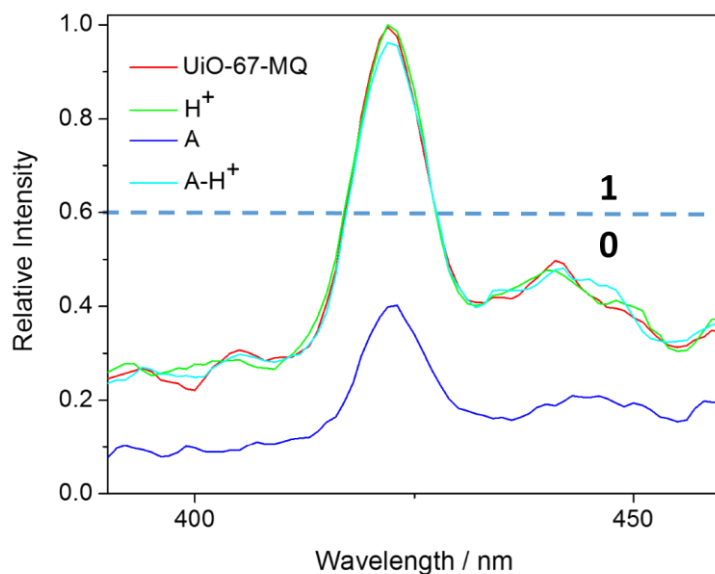


Figure S20. Fluorescence spectra of UiO-67-DQ for INHIBIT and IMPLICATION gates.

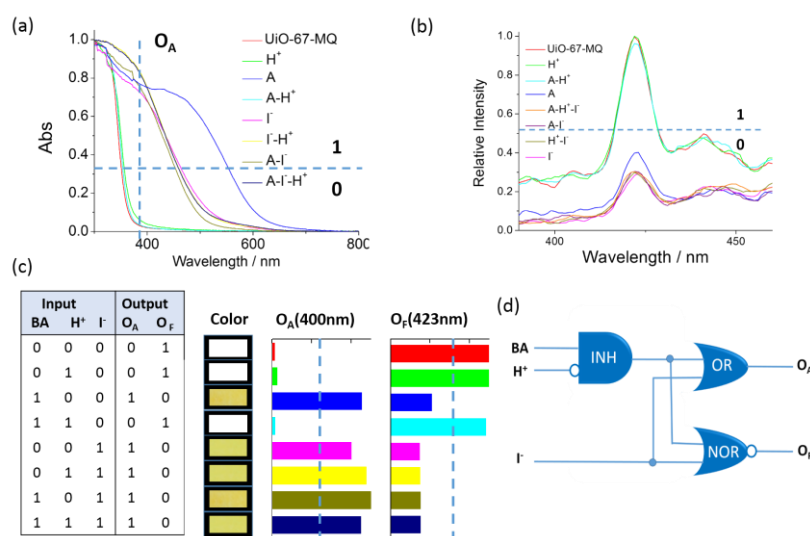


Figure S21. UiO-67-MQ-based 3-input operation integrating INHIBIT and OR/NOR logic gates based with BA (BA = butylamine), H⁺ and I⁻ as inputs. (a) UV-Vis spectra measured with test papers for different input combinations. (b) Fluorescence spectra for different input combinations. (c) Truth table, pictures of the test papers and column plots for different outputs. (d) Logic circuits.

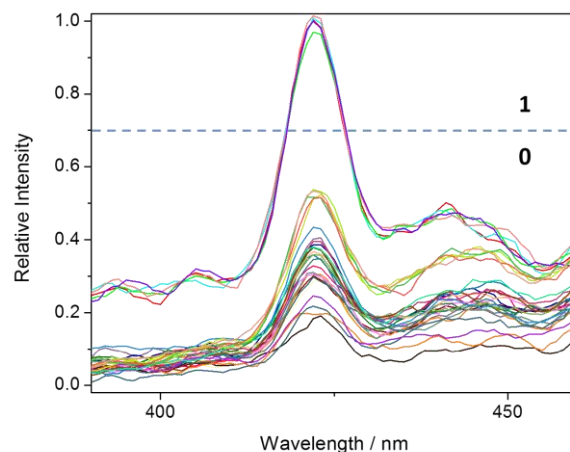


Figure S22. Fluorescence spectra of UiO-67-MQ for different input combinations of the 5-input logic circuit successively integrating OR, INHIBIT and NOR gates.

References

- (1) Rama, G.; Arda, A.; Marechal, J.-D.; Gamba, I.; Ishida, H.; Jimenez-Barbero, J.; Vazquez, M. E.; Vazquez Lopez, M. Stereoselective Formation of Chiral Metallopeptides. *Chem. - Eur. J.* **2012**, *18*, 7030-7035.
- (2) Nickerl, G.; Leistner, M.; Helten, S.; Bon, V.; Senkovska, I.; Kaskel, S. Integration of Accessible Secondary Metal Sites into MOFs for H₂S Removal. *Inorg. Chem. Front.* **2014**, *1*, 325-330.
- (3) Yang, N. N.; Sun, W.; Xi, F. G.; Sui, Q.; Chen, L. J.; Gao, E. Q. Postsynthetic N-Methylation Making a Metal-Organic Framework Responsive to Alkylamines. *Chem. Commun.* **2017**, *53*, 1747-1750.
- (4) Kuroboshi, M.; Kondo, T.; Tanaka, H. Diquat Derivatives, a Precursor of Organic Reductant. *Heterocycles* **2015**, *90*, 723-729.
- (5) Karaca, E.; Kaplan Can, H.; Bozkaya, U.; Oezcicek Pekmez, N. Charge-Transfer Complex of P-Aminodiphenylamine with Maleic Anhydride: Spectroscopic, Electrochemical, and Physical Properties. *Chemphyschem* **2016**, *17*, 2056-2065.
- (6) Cardona, C. M.; Li, W.; Kaifer, A. E.; Stockdale, D.; Bazan, G. C. Electrochemical Considerations for Determining Absolute Frontier Orbital Energy Levels of Conjugated Polymers for Solar Cell Applications. *Adv Mater* **2011**, *23*, 2367-2371.